Nematic quantum critical point without magnetism in $FeSe_{1-x}S_x$ superconductors

Suguru Hosoi[a], Kohei Matsuura[a], Kousuke Ishida[a], Hao Wang[a], Yuta Mizukami[a], Tatsuya Watashige[b], Shigeru Kasahara[b], Yuji Matsuda[b], and Takasada Shibauchi[a,1]

[a]Department of Advanced Materials Science, University of Tokyo, Kashiwa, Chiba 277-8561, Japan; [b]Department of Physics, Kyoto University, Sakyo-ku, Kyoto 606-8502, Japan

This manuscript was compiled on July 1, 2016

In most unconventional superconductors, the importance of antiferromagnetic fluctuations is widely acknowledged. In addition, cuprate and iron-pnictide high-temperature superconductors often exhibit unidirectional (nematic) electronic correlations, including stripe and orbital orders, whose fluctuations may also play a key role for electron pairing. In these materials, however, such nematic correlations are intertwined with antiferromagnetic or charge orders, preventing us to identify the essential role of nematic fluctuations. This calls for new materials having only nematicity without competing or coexisting orders. Here we report systematic elastoresistance measurements in $FeSe_{1-x}S_x$ superconductors, which, unlike other iron-based families, exhibit an electronic nematic order without accompanying antiferromagnetic order. We find that the nematic transition temperature decreases with sulfur content x, whereas the nematic fluctuations are strongly enhanced. Near $x \approx 0.17$, the nematic susceptibility diverges towards absolute zero, revealing a nematic quantum critical point. The obtained phase diagram for the nematic and superconducting states highlights $FeSe_{1-x}S_x$ as a unique nonmagnetic system suitable for studying the impact of nematicity on superconductivity.

electronic nematicity| iron-based superconductors | nematic susceptibility | unconventional superconductivity

The prime candidate for the unconventional mechanism of superconductivity in many strongly correlated electron systems including cuprate, iron-based, and heavy-fermion superconductors is based on magnetic fluctuations [? ? ? ?]. In these materials, dome-shaped superconducting phases appear in the vicinity of end point of the antiferromagnetic (AFM) order, where spin fluctuations are strongly enhanced. Recently, however, other competing or coexisting orders that break rotational symmetry of the system have been frequently found in these materials [? ? ? ?], and the importance of fluctuations of these orders on superconducting pairing has been suggested theoretically [? ? ? ?].

In underdoped cuprate superconductors, unidirectional electronic correlations (stripe correlations) appear in the pseudogap state, whose relation with superconductivity is a center of debate. It has become more complicated after the charge density wave (CDW) order has been observed in a portion of this pseudogap region of the phase diagram [?]. In iron pnictides, the tetragonal-to-orthorhombic structural transition always precedes or coincides with the AFM transition [?]. Below the structural transition temperature T_s, electronic nematicity that represents a large electronic anisotropy breaking the C_4 rotational symmetry, is observed [?], which may have a similar aspect with the stripe correlations in underdoped cuprates. In both cases, however, the nematicity is largely coexisting and intertwined with other CDW and AFM orders. Large nematic fluctuations have been experimentally observed in $BaFe_2As_2$ systems above T_s, and these nematic fluctuations are strikingly enhanced with approaching the end point of the structural transition [? ?]. This suggests the presence of a nematic quantum critical point (QCP), but in this case the nematic QCP coincides with, or locates very close to the AFM QCP, where antiferromagnetic fluctuations are also enhanced [?]. This raises a fundamental question as to which fluctuations are the main driving force of the Cooper pairing in this system.

Recently there is growing evidence that the iron-chalcogenide FeSe [?] displays remarkable properties. The superconducting transition temperature of $T_c = 9\,K$ at ambient pressure is largely enhanced up to 38 K under pressure [?]. Further enhancement of T_c has been reported in monolayer FeSe [?]. What is important in this system is that despite its high nematic transition temperature of $T_s \approx 90\,K$ [?], no magnetic order occurs down to $T \to 0\,K$. Above T_s, large nematic fluctuations are reported but, unlike iron pnictides, no sizable AFM fluctuations are observed [?]. The enhanced nematic fluctuations most likely have an orbital origin, because a momentum-dependent orbital polarization has been found in angle-resolved photoemission spectroscopy in the nematic phase below T_s [?]. More recently, it has been shown that the high-energy spin excitations measured by the inelastic neutron scattering do not show significant tempera-

Significance Statement

The electronic nematic order that spontaneously breaks rotational symmetry of the system, is perhaps one of the most surprising states of matter. A key issue is the relationship between the fluctuations of such nematic order and high-temperature superconductivity in cuprates and iron-pnictides. However, because of coexisting antiferromagnetic or charge-density-wave orders, it is difficult to pinpoint the impact of nematic fluctuations on superconductivity. Here we report a quantum critical point (QCP) of pure nematic order without accompanying other orders in $FeSe_{1-x}S_x$ superconductors. We find that the nematic fluctuations are divergently enhanced at the nematic QCP. This discovery opens up a new avenue to study the unconventional superconductivity mediated by exotic mechanisms different from the well-studied spin fluctuations.

T.S. designed research; S.H., K.M., K.I., H.W., Y. Mizukami, T.W., S.K., Y. Matsuda, and T.S. performed research; S.H. and T.S. analyzed data; and S.H., S.K., Y. Matsuda, and T.S. wrote the paper.

The authors declare no conflict of interest

[1]To whom correspondence should be addressed. E-mail: shibauchi@k.u-tokyo.ac.jp

ture dependence above T_s [?], which indicates no direct correlations between dynamical spin susceptibility $\chi(\mathbf{q}, T)$ and the nematic susceptibility, inconsistent with the spin-nematic scenario [?]. Although these results imply that the nematic transition in FeSe is orbital driven, the most important issue, namely the presence of a nonmagnetic nematic QCP at which the nematic fluctuation diverges with $T \to 0\,$K, remains open. The presence or absence of such a QCP should provide pivotal information on the superconductivity of iron-based high-T_c materials. It has been shown very recently that the applying pressure leads to the suppression of T_s, but near the critical pressure at which T_s vanishes, the magnetic ordering is induced [? ? ?], preventing our understanding of the interplay between nematicity and superconductivity.

Recent advances in the crystal growth of iron chalcogenides by using the chemical vapour transport technique [? ?] allow us to grow high-quality single crystals of $FeSe_{1-x}S_x$. The high quality of the obtained crystals is evidenced by the low residual resistivity and the observation of quantum oscillations [? ?]. Here we report that the partial substitution of isoelectric S for the Se site [? ? ? ?] leads to the complete suppression of this nematic transition without inducing the AFM order. Moreover T_c shows a maximum at $x \approx 0.08$ in $FeSe_{1-x}S_x$, suggesting the presence of superconducting dome, but the detailed phase diagram has some differences from those in $BaFe_2As_2$-based systems with AFM QCP. Therefore $FeSe_{1-x}S_x$ appears to be a key material to investigate relationship between the nonmagnetic nematic fluctuations and the superconductivity.

Results and Discussions

The temperature dependence of the in-plane resistivity $\rho(T)$ in these high-quality crystals shows a kink at the nematic transition at T_s, which is gradually decreased to lower temperatures with S substitution (Fig. 1*A*). At high concentrations $x \geq 0.17$, the kink anomaly of $\rho(T)$ disappears, which is more clearly seen in the temperature derivative $\mathrm{d}\rho/\mathrm{d}T(T)$ (Fig. 1*B*). In contrast to the physical pressure case where another clear anomaly at a temperature different from T_s is reported indicating the appearance of a magnetic transition, we find no such anomaly in the entire x range of this study, which implies that the ground states of this system are nonmagnetic up to at least $x = 0.21$.

An elegant way to evaluate experimentally the nematic fluctuations has been developed by the Stanford group, that is based on the elastoresistance measurements by using a piezoelectric device [? ?]. We utilize this technique in our $FeSe_{1-x}S_x$ to extract the temperature dependence of the so-called nematic susceptibility $\chi_{\rm nem}$. Here the change in the resistance $N \sim (\Delta R/R)$ induced by the strain that can be controlled by the voltage applied to the piezoelectric device is measured as a function of strain ϵ (Fig. 2*A*). This quantity N is proportional to the nematic order parameter, and thus its fluctuations can be quantified by the nematic susceptibility $\chi_{\rm nem} \sim \frac{\partial N}{\partial \epsilon}$, which is given by the slope of the $(\Delta R/R)$ versus ϵ curve [?]. To cancel the effect of anisotropic strain induced in the piezoelectric device (the Poisson effect) [?], we measured the resistance changes $(\Delta R/R)_{xx}$ and $(\Delta R/R)_{yy}$ for two current directions orthogonal each other in FeSe ($x = 0$) crystals (Figs. 2*A*, *B*). The nematic susceptibility data obtained from the combination of $(\Delta R/R)_{xx}$ and $(\Delta R/R)_{yy}$ are essentially identical to those from $(\Delta R/R)_{xx}$ alone (Fig. 3*A*). Therefore, we measure only $(\Delta R/R)_{xx}$ for substituted samples $x > 0$ to avoid the effect of small difference of the composition x in different crystals from the same batch. The sign of the nematic susceptibility above T_s is positive, which corresponds to the positive value of $\rho_a - \rho_b$ where a and b represent the orthorhombic crystal axes ($a > b$). This positive sign is consistent with the previous results in FeSe [? ?] and $FeTe_{0.6}Se_{0.4}$ [?], but is opposite to the Co-doped $BaFe_2As_2$ case [?]. This sign difference may be related to the difference of Fermi surface structure in different materials. In hole-doped $BaFe_2As_2$ materials, the doping-induced sign reversal of $\rho_a - \rho_b$ has been observed and the importance of anisotropic quasiparticle scattering in the nematic state has been suggested [?]. More recently, however, the optical analysis indicates that the anisotropy of Drude spectral weight, which is related to the detailed Fermi surface structure and effective mass, is more essential than the scattering rate to determine the resistive anisotropy [?]. In the case of FeSe, the Fermi surface in the nematic state has several unusual features including the smallness of Fermi energies [? ?], and different anisotropy between hole and electron bands [?], which may be relevant for the observed positive sign of $\rho_a - \rho_b$.

The temperature dependence of the obtained nematic susceptibility shows a systematic trend as a function of the sulfur content x (Figs. 3*A*-*E*). In the tetragonal state above T_s, $\chi_{\rm nem}(T)$ can be fitted to the Curie-Weiss type temperature dependence given by

$$\chi_{\rm nem} = \frac{\lambda}{a(T - T_\theta)} + \chi^0, \qquad [1]$$

where λ and a are constants, and T_θ is the Weiss temperature, which represents the electronic nematic transition temperature without the lattice coupling. The observed changes in the resistance is given by $\Delta R/R = \Delta\rho/\rho + \Delta L/L - \Delta A/A$, the last two terms on the right hand side represent geometric factors related to changes in the length L and cross-sectional area A [?]. These terms contribute to the temperature-independent term χ^0 in Eq. (1), which is dominant in simple metals. In the present $FeSe_{1-x}S_x$ system, however, $\chi_{\rm nem}(T)$ has strong temperature dependence, indicating that nematic fluctuations are very large. With a proper choice of χ^0, $1/(\chi_{\rm nem} - \chi^0)$ follows nearly T-linear dependence in a wide temperature range of the tetragonal phase, consistent with the Curie-Weiss law (Eq. [1]).

The obtained phase diagram based on our single-crystal study is shown in Fig. 4. The nematic transition temperature T_s monotonically decreases and vanishes at $x \gtrsim 0.17$. The Weiss temperature T_θ crosses the zero line and changes sign at $x \approx 0.17$, where the magnitude of $\chi_{\rm nem}$ is strongly enhanced. These results provide clear evidence that the nematic QCP is present near this composition $x = 0.17$, where nematic fluctuations are diverging toward $T \to 0\,$K. We stress that the present measurements are performed under identical conditions in a series of samples with similar dimensions and thus the obtained systematic results represent intrinsic properties of this system.

Near the QCP, the $\chi_{\rm nem}(T)$ data exhibit some deviations from the Curie-Weiss temperature dependence (gray regions in Figs. 3*B*-*E*, *G*-*J*). Such deviations have also been frequently found in iron-based superconductors when T_s becomes low [?]. The origin of these deviations from the Curie-Weiss law has not been fully understood, but one should consider possible effects of impurity scattering that may be modified by quantum criticality. In the theory of magnetic quantum critical point, various physical quantities show non-Fermi liquid behavior, and magnetic susceptibility may deviate from the Curie-Weiss law [?]. Magnetic susceptibility directly couples to the correlation length, which depends on dimension and dynamical exponent of the system according to the Hertz-Millis theory [?]. In analogy to this, the nematic correlation length in the presence of disorder would have some characteristic temperature dependence different from the Fermi-liquid behaviors, and then the deviations from Curie-Weiss law may be expected in the nematic susceptibility. When the effects of disorder is strong, it has been discussed that the so-called Griffith singularity may occur, which modifies the critical behavior [?]. In any case, these disorder effects should weaken the divergent behavior especially near the QCP, which is consistent with our results.

The present results provide evidence that a nonmagnetic nematic QCP lies in the superconducting phase, which has the same topology as the phase diagrams of iron pnictides [?] and heavy fermions [?] in which AFM QCP locates inside the superconducting dome. However, this nematic QCP has several different aspects from the well-studied AFM QCP. First, the resistivity data (Fig. 1*A*) shows non-T^2 dependence for all the samples we measured, and we find no significant enhancement in the residual resistivity near the nematic QCP, which appears to be different from the expectations in the magnetic QCP case [?]. Second, in iron pnictides T_c shows the maximum at around the AFM QCP [?], whereas in the present system T_c shows a maximum deep inside the nematic ordered phase, not at the nematic QCP. This suggests that the critical nematic fluctuations do not have simple correlations with the T_c enhancement, although some theoretical calculations propose a T_c peak at a nematic QCP [?]. These results highlight the apparent insensitivity of fermionic properties including superconductivity to the nematic quantum criticality, which shows a strong contrast to the AFM criticality. One may consider that the AFM fluctuations have more direct coupling to superconductivity or that the combination of AFM and nematic fluctuations is important to enhance superconductivity.

Possible origins of these unexpected results are related to the fact that the nematic order is most likely a ferro-type order with the wave vector $\mathbf{q} = 0$ [? ?], which is different from AFM order with a finite $\mathbf{q}$. In a ferro-type order, the Fermi surface change is not as dramatic as in the antiferro-type order in which band-folding occurs, and thus the competition between superconductivity and ferro-nematic order may be much more modest. Indeed, the unusual lack of coupling between superconductivity and orthorhombic distortion in nonmagnetic FeSe has been reported by the thermal expansion measurements [?]. Another factor which may be relevant here is the enhanced quasiparticle damping (depairing) effect near a ferro-type QCP, that can suppress T_c. In fact, such a scenario has been discussed in ferromagnetic superconductors, such as UGe_2, in which the peak of the T_c dome is not located at a ferromagnetic end point [?]. However, the resistivity curves do not show a dramatic change near the present nematic QCP, and thus further studies are necessary to clarify this point.

It should be noted that in cuprate superconductors the importance of nematic electronic correlations has been suggested as well [? ?], and the quantum criticality of the CDW or the pseudogap phase has been discussed [?]. In $YBa_2Cu_3O_{7-\delta}$ [?] and $YBa_2Cu_4O_8$ [?], however, opposite correlations between T_c and the quasiparticle mass enhancement associated with the putative quantum phase transition have been reported, causing controversy on the relationship between quantum fluctuations and superconductivity in cuprates. To solve this issue it would be important to separate the effects of CDW order from the nematic correlations in the pseudogap state.

Finally, we should add that in iron-based superconductors the multi-orbital degrees of freedom of Fe 3*d* electrons are essential in forming orbital ordering, which is quite different from the cuprate case. However, the recent theoretical study suggests that in cuprates the nematic CDW-like correlations involving the Cu 3*d* and O 2*p* orbitals may be considered as intra-unit-cell orbital order [?]. Therefore the nematicity in these strongly correlated electron systems may have rather general grounds involving orbital physics. Thus the present discovery of the nematic QCP and enhanced ferro-type nematic fluctuations without coexisting or competing magnetic order in $FeSe_{1-x}S_x$ can provide a unique avenue to study the unconventional superconductivity mediated by exotic mechanisms other than spin fluctuations.

Materials and Methods

Single crystals of $FeSe_{1-x}S_x$ were grown by the chemical vapour transport technique. A mixture of Fe, Se and S powders together with KCl and $AlCl_3$ powders was sealed in an evacuated SiO_2 tube. The ampule was heated to $390-450^\circ$C on one end while the other end was kept at $140-200^\circ$C. In these conditions, we were able to cover a much wider x range than previous single crystal studies [? ?], which is important to completely suppress the nematic transition. The actual sulfur composition x is determined by the energy dispersive X-ray spectroscopy, and is found to be about 80% of the nominal S content (Fig. 1*A*, inset). The experimental setup for the measurement of nematic susceptibility χ_{nem} is shown in the inset of Fig. 2 [?]. The samples are cut into bar-shape along the orthogonal crystal axis (tetragonal [110]) and are glued on a piezoelectric stack. After mounted on the piezoelectric stack, samples are cleaved so that the thickness becomes about $\sim 30\,\mu$m and the strain is sufficiently transmitted to them. The strain $\epsilon = \frac{\Delta L}{L}$ is induced by applying the voltage to piezoelectric stack and measured by a strain gauge glued to the surface of piezoelectric stack. We simultaneously measure the changes in the resistance when varying the strain and this induced anisotropy directly couples to the electronic nematic order parameter.

ACKNOWLEDGMENTS. We thank J.-H. Chu, A. I. Coldea, R. M. Fernandes, I. R. Fisher, C. W. Hicks, S. Kawachi, H. Kontani, S. Lederer, A. H. Nevidomskyy, T. Takimoto, M. Tokunaga, M. D. Watson, and T. Wolf for helpful comments and discussions. This work was supported by Grants-in-Aid for Scientific Research (KAKENHI) from Japan Society for the Promotion of Science (JSPS), and by the 'Topological Material Science' Grant-in-Aid for Scientific Research on Innovative Areas from the Ministry of Education, Culture, Sports, Science and Technology (MEXT) of Japan.

1. Moriya T, Ueda K (2003) Antiferromagnetic spin fluctuation and superconductivity. *Rep Prog Phys* 66(8):1299-1341.
2. Scalapino DJ (2012) A common thread: the pairing interaction for the unconventional superconductors. *Rev Mod Phys* 84(4):1383-1417.
3. Hirschfeld PJ, Korshunov MM, Mazin II (2011) Gap symmetry and structure of Fe-based superconductors. *Rep Prog Phys* 74(12):124508.
4. v Löhneysen H, Rosch A, Vojta M, Wölfle P (2007) Fermi-liquid instabilities at magnetic quantum phase transitions. *Rev Mod Phys* 79(3):1015-1075.
5. Keimer B, Kivelson SA, Norman MR, Uchida S, Zaanen J (2015) From quantum matter to high-temperature superconductivity in copper oxides. *Nature* 518(7538), 179-186.
6. Fradkin E, Kivelson SA, Tranquada JM (2015) Theory of intertwined orders in high temperature superconductors. Rev Mod Phys 87(2):457-482.
7. Fernandes RM, Chubukov AV, Schmalian J (2014) What drives nematic order in iron-based superconductors? *Nat Phys* 10(2):97-104.
8. Shibauchi T, Ikeda H, Matsuda Y (2014) Broken symmetries in URu_2Si_2. *Philo. Mag.* 94(32-33): 3747-3759.
9. Maier TA, Scalapino DJ (2014) Pairing interaction near a nematic quantum critical point of a three-band CuO_2 model. *Phys Rev B* 90(17):174510.
10. Metlitski MA, Mross DF, Sachdev S, Senthil T (2015) Cooper pairing in non-Fermi liquids. *Phys Rev B* 91(11):115111.
11. Lederer S, Schattner Y, Berg E, Kivelson SA (2015) Enhancement of superconductivity near a nematic quantum critical point. *Phys Rev Lett* 114(9):097001.
12. Kontani H, Onari S (2012) Orbital-fluctuation-mediated superconductivity in iron pnictides: analysis of the five-orbital Hubbard-Holstein model. *Phys Rev Lett* 104(15):157001.
13. Kuo H-H, Chu J-H, Palmstrom JC, Kivelson SA, Fisher IR (2016) Ubiquitous signatures of nematic quantum criticality in optimally doped Fe-based superconductors. *Science* 352(6288):958-962.
14. Yoshizawa M, et al. (2012) Structural quantum criticality and superconductivity in iron-based superconductor $Ba(Fe_{1-x}Co_x)_2As_2$. *J Phys Soc Jpn* 81(2):024604.
15. Shibauchi T, Carrington A, Matsuda Y (2014) A quantum critical point lying beneath the superconducting dome in iron-pnictides. *Annu Rev Condens Matter Phys* 5:113-135.
16. Hsu F-C, et al. (2008) Superconductivity in the PbO-type structure α-FeSe. *Proc Natl Acad Sci USA* 105(38):14262-14264.
17. Sun JP, et al. (2016) Dome-shaped magnetic order competing with high-temperature superconductivity at high pressures in FeSe. *Nat. Commun* 7:12146.
18. Wang Q-Y, et al. (2012) Interface-induced high-temperature superconductivity in single unit-cell FeSe films on $SrTiO_3$. *Chin Phys Lett* 29(3):037402.
19. Böhmer AE, et al. (2013) Lack of coupling between superconductivity and orthorhombic distortion in stoichiometric single-crystalline FeSe. *Phys Rev B* 87(18):180505(R).
20. Baek S-H, et al. (2015) Orbital-driven nematicity in FeSe. *Nat Mater* 14(2):210-214.
21. Suzuki Y, et al. (2015) Momentum-dependent sign inversion of orbital order in superconducting FeSe. *Phys Rev B* 92(20):205117.
22. Shamoto S, et al. (2015) Spin nematic susceptibility studied by inelastic neutron scattering in FeSe. arXiv:1511.04267.
23. Bendele M, et al. (2012) Coexistence of superconductivity and magnetism in $FeSe_{1-x}$ under pressure. *Phys Rev B* 85(6):064517.
24. Terashima T, et al. (2015) Pressure-induced antiferromagnetic transition and phase diagram in FeSe. *J Phys Soc Jpn* 84(6):063701.
25. Kasahara S, et al. (2014) Field-induced superconducting phase of FeSe in the BCS-BEC cross-over. *Proc Natl Acad Sci USA* 111(46):16309-16313.
26. Terashima T, et al. (2014) Anomalous Fermi surface in FeSe seen by Shubnikov-de Haas oscillation measurements. *Phys Rev B* 90(14):144517.
27. Watson MD, et al. (2015) Dichotomy between the hole and electron behaviour in multiband superconductor FeSe probed by ultrahigh magnetic fields *Phys Rev Lett* 115(2):027006.
28. Mizuguchi Y, Tomioka F, Tsuda S, Yamaguchi T, Takano Y (2009) Substitution effects on FeSe superconductor. *J Phys Soc Jpn* 78(7):074712.
29. Guo J, Lei H, Hayashi F, Hosono H (2014) Superconductivity and phase instability of NH_3-free Na-intercalated $FeSe_{1-z}S_z$. *Nat Commun* 5:4756.
30. Watson MD, et al. (2015) Suppression of orbital ordering by chemical pressure in $FeSe_{1-x}S_x$. *Phys Rev B* 92(12):121108(R).
31. Moore SA, et al. (2015) Evolution of the superconducting properties in $FeSe_{1-x}S_x$. *Phys Rev B* 92(23):235113.
32. Chu J-H, Kuo H-H, Analytis JG, Fisher IR (2012) Divergent nematic susceptibility in an iron arsenide superconductor. *Science* 337(6095):710-712.
33. Kuo H-H, Shapiro MC, Riggs SC, Fisher IR (2013) Measurement of the elastoresistivity coefficients of the underdoped iron arsenide $Ba(Fe_{0.975}Co_{0.025})_2As_2$. *Phys Rev B* 88(8):085113.
34. Tanatar MA, et al. (2015) Origin of the resistivity anisotropy in the nematic phase of FeSe. arXiv:1511.04757.
35. Blomberg EC, et al. (2013) Sign-reversal of the in-plane resistivity anisotropy in hole-doped iron pnictides. *Nat Commun* 4:1914.
36. Mirri C, et al. (2016) Electrodynamic response in the electronic nematic phase of $BaFe_2As_2$. *Phys Rev B* 93(08):085114.
37. Lee C-C, Yin W-G, Ku W (2009) Ferro-orbital order and strong magnetic anisotropy in the parent compounds of iron-pnictide superconductors. *Phys Rev Lett* 103(26):267001.
38. Lv W, Wu J, Phillips P (2009) Orbital ordering induces structural phase transition and the resistivity anomaly in iron pnictides. *Phys Rev B* 80(22):224506.
39. Saxena SS, et al. (2000) Superconductivity on the border of itinerant-electron ferromagnetism in UGe_2. *Nature* 406(6796):587-592.
40. Ramshaw BJ, et al. (2015) Quasiparticle mass enhancement approaching optimal doping in a high-T_c superconductor. *Science* 348(6232):317-320.
41. Putzke C, et al. (2016) Inverse correlation between quasiparticle mass and T_c in a cuprate high-T_c superconductor. *Sci Adv* 2(3):e1501657.
42. Yamakawa Y, Kontani H (2015) Spin-fluctuation-driven nematic charge-density wave in cuprate superconductors: Impact of Aslamazov-Larkin vertex corrections. *Phys Rev Lett* 114(25):257001.

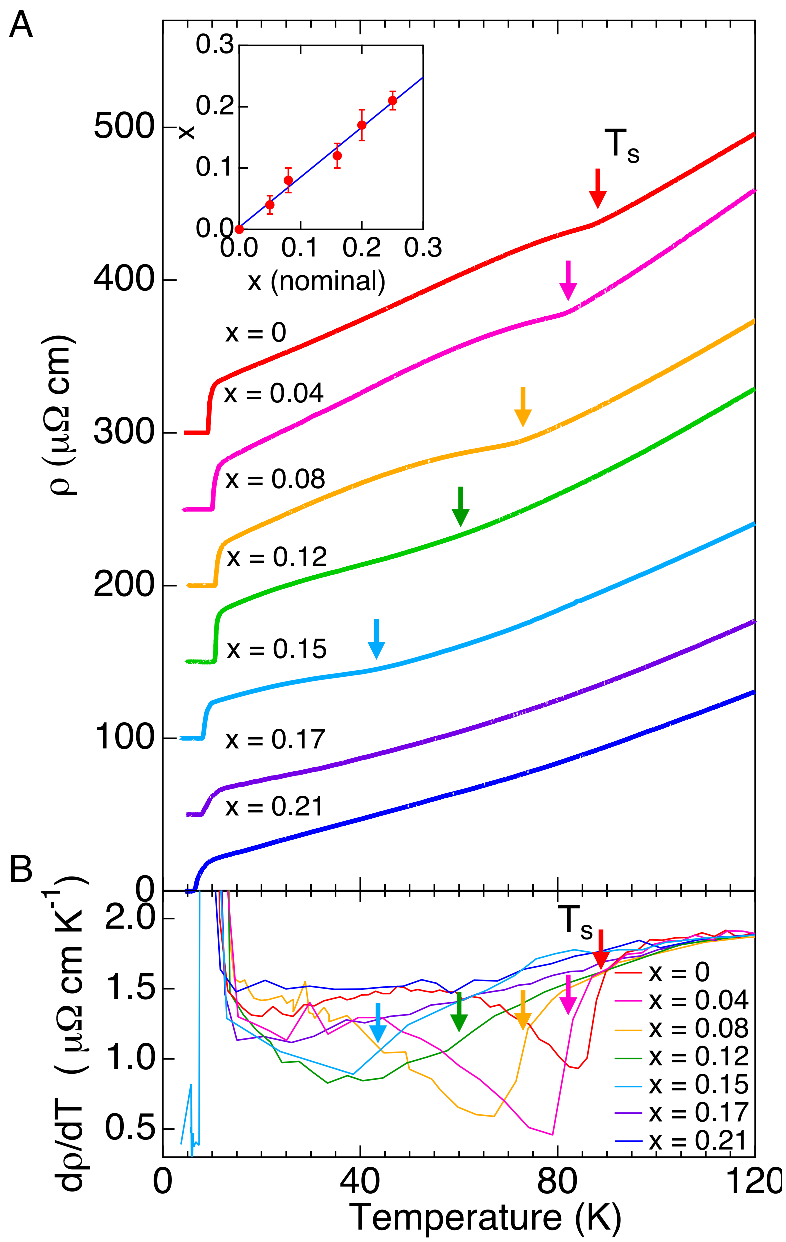

Fig. 1. Temperature dependence of resistivity in $FeSe_{1-x}S_x$ single crystals. (A) In-plane resistivity ρ as a function of temperature in several crystals with different x. Each curve is shifted vertically for clarity. Sulfur content x determined by energy dispersive X-ray spectroscopy is linearly proportional to the nominal composition (inset). (B) Temperature dependence of $\mathrm{d}\rho/\mathrm{d}T$. Each curve is shifted vertically so that all the data at 120 K merge. The arrows indicate the nematic (structural) transition temperature T_s estimated from the inflection point, which is more accurately determined by the peak position in the temperature dependence of the nematic susceptibility (Figs. 3A-C).

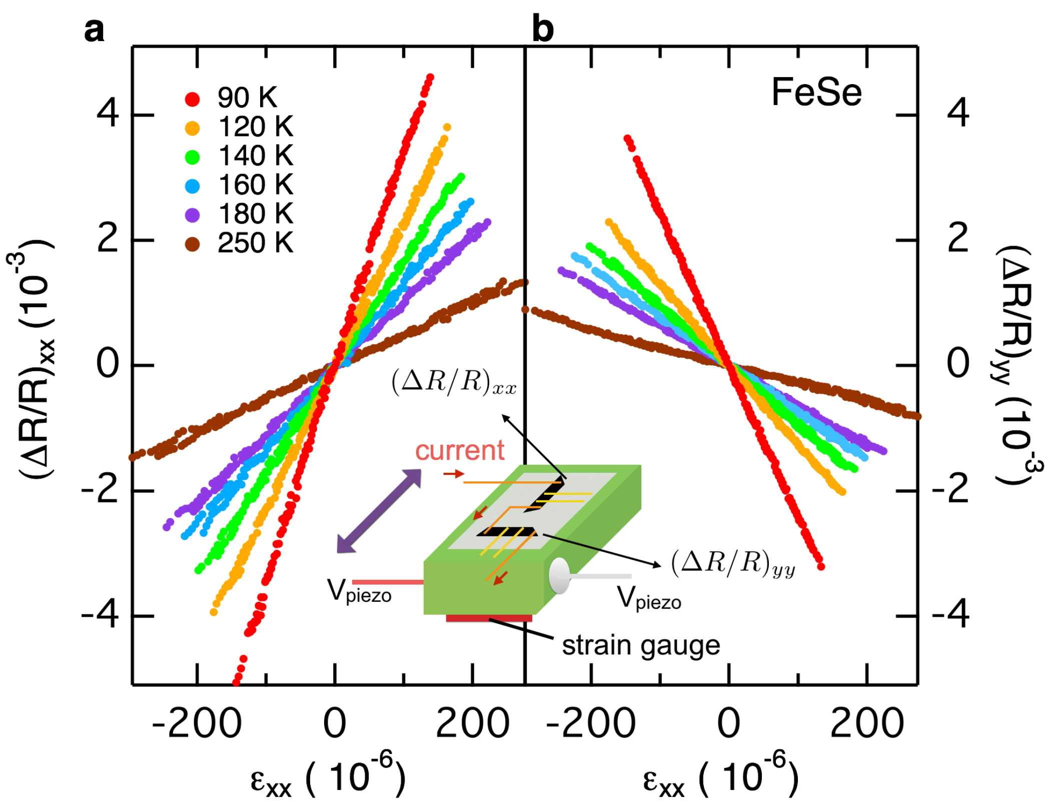

Fig. 2. Elastoresistance measurements by using the piezoelectric device. (A) Relative change in the resistance of an FeSe crystal at several temperatures above $T_{\rm s}$ as a function of strain induced by the attached piezoelectric stack. The current direction in the crystal is parallel to the strain direction. (B) Similar data for another crystal in which the current direction in perpendicular to the strain direction. Inset is a schematic experimental set-up. The crystals (black bars) are attached on top of the piezoelectric stack (green) which expands (shrinks) along the violet arrows when positive (negative) bias is applied. The strain is measured by a strain gauge (red) attached underneath the device.

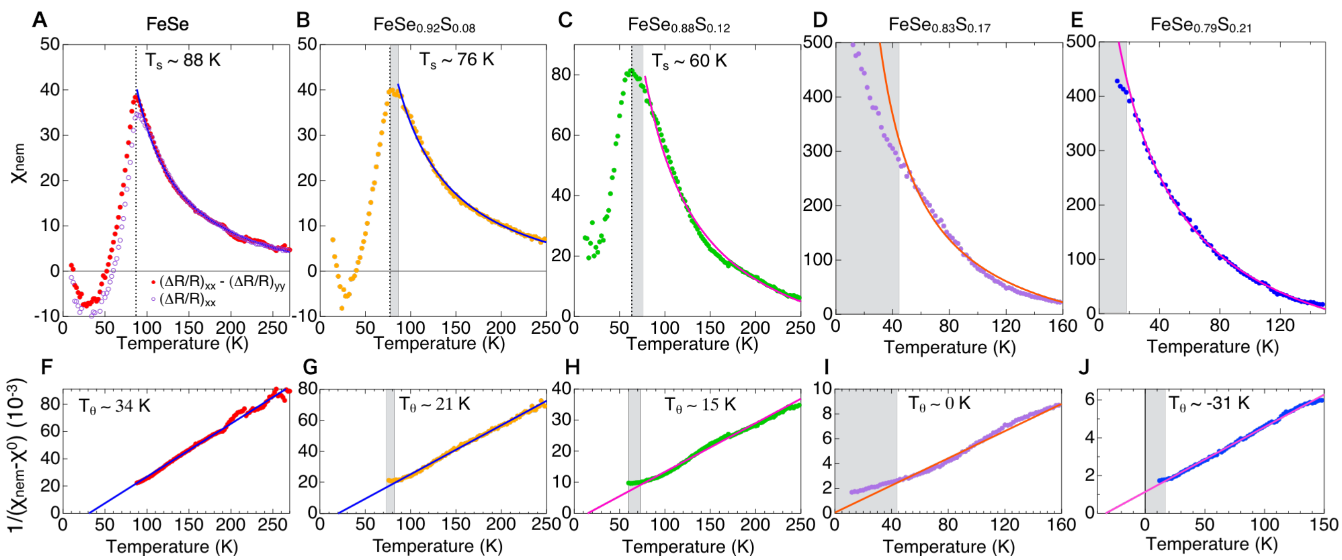

Fig. 3. Divergent nematic susceptibility in $FeSe_{1-x}S_x$ single crystals. (*A*-*E*) Temperature dependence of the nematic susceptibility $\chi_{\rm nem}$ for $x = 0$ (*A*), 0,08 (*B*), 0.12 (*C*), 0.17(*D*), and 0.21 (*E*). In FeSe ($x = 0$), the nematic susceptibility data extracted by using both $(\Delta R/R)_{xx} - (\Delta R/R)_{yy}$ (red filled circles) and $(\Delta R/R)_{xx}$ (violet open circles) show consistent results. For other $x > 0$ samples only $(\Delta R/R)_{xx}$ data has been used (*B*-*E*). (*F*-*J*) Temperature dependence of inverse of $\chi_{\rm nem} - \chi^0$ for $x = 0$ (*F*), 0,08 (*G*), 0.12 (*H*), 0.17(*I*), and 0.21 (*J*). Here χ^0 is a temperature independent constant, coming from the geometrical change that leads to a resistance change under strain. Solid lines are the fits of $\chi_{\rm nem} - \chi^0$ to the Curie-Weiss law $\propto 1/(T - T_\theta)$, and the obtained values of the Weiss temperature T_θ are indicated. The nematic transition is defined by the peak in $\chi_{\rm nem}(T)$, which is quantitatively consistent with the kink anomaly in $\rho(T)$ curves (Fig. 1). In the temperature range highlighted in grey, the nematic susceptibility data above $T_{\rm s}$ shows some deviations from the Curie-Weiss law.

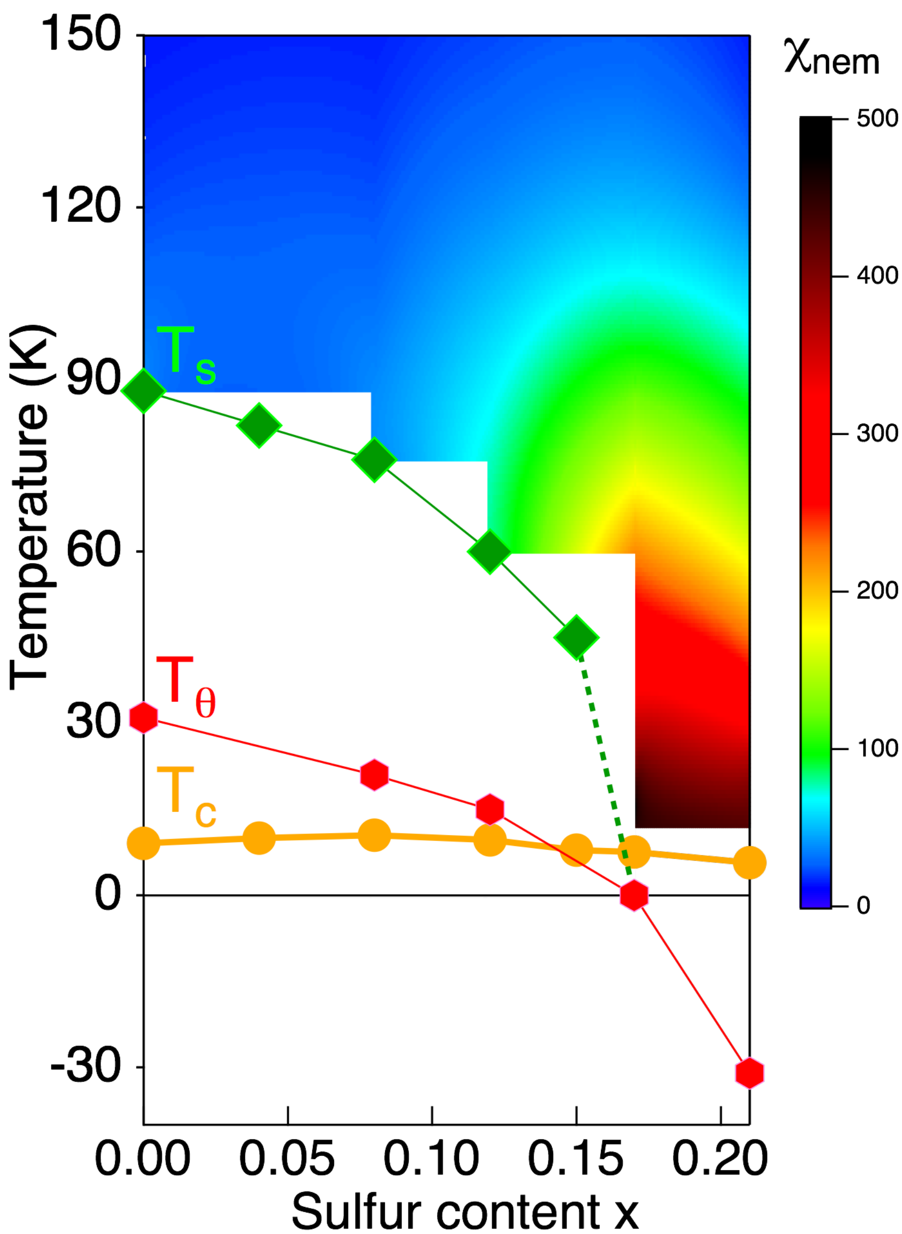

Fig. 4. Phase diagram and quantum criticality in FeSe$_{1-x}$S$_x$. Temperature dependence of the nematic transition (T_s, green diamonds) and the superconducting transition temperature (T_c, orange circles) determined by the zero resistivity criteria. The Weiss temperature obtained by the Curie-Weiss analysis of the nematic susceptibility data (Fig. 3) is also plotted (T_θ, red hexagons). The magnitude of $\chi_{\rm nem}$ in the tetragonal phase is superimposed in the phase diagram by a colour contour (see the colour bar for the scale). The lines are the guides for the eyes.